NIH Public Access
Author Manuscript
Hepatology. Author manuscript; available in PMC 2011 January 1.

Published in final edited form as:
Hepatology. 2010 January ; 51(1): 181–190. doi:10.1002/hep.23265.

Mouse organic solute transporter α deficiency enhances renal excretion of bile acids and attenuates cholestasis

Carol J. Soroka[1], **Albert Mennone**[1], **Lee R. Hagey**[2], **Nazzareno Ballatori**[3], and **James L. Boyer**[1]

[1]Yale Liver Center, Yale University School of Medicine, New Haven, CT 06520

[2]Department of Medicine, University of California at San Diego, San Diego, CA 92103

[3]Dept of Environmental Medicine, University of Rochester School of Medicine, Rochester, NY 14642

Abstract

Organic solute transporter alpha-beta (Ostα-Ostβ) is a heteromeric bile acid and sterol transporter that facilitates the entero- and renal-hepatic circulation of bile acids. Hepatic expression of this basolateral membrane protein is increased in cholestasis, presumably to facilitate removal of toxic bile acids from the liver. In this study we show that the cholestatic phenotype induced by common bile duct ligation (BDL) is reduced in mice genetically deficient in *Ostα*. Although *Ostα*$^{-/-}$ mice have a smaller bile acid pool size which could explain lower serum and hepatic levels of bile acids after BDL, gallbladder bilirubin and urinary bile acid concentrations were significantly greater in *Ostα*$^{-/-}$ BDL mice, suggesting additional alternative adaptive responses. Livers of *Ostα*$^{-/-}$ mice had higher mRNA levels of constitutive androstane receptor (Car) than wild-type BDL mice and increased expression of Phase I enzymes (*Cyp7a1*, *Cyp2b10*, *Cyp3a11*), Phase II enzymes (*Sult2a1*, *Ugt1a1*) and Phase III transporters *(Mrp2*, *Mrp3*). Following BDL, the bile acid pool size increased in *Ostα*$^{-/-}$ mice and protein levels for the hepatic basolateral membrane export transporters, Mrp3 and Mrp4, and for the apical bilirubin transporter, Mrp2, were all increased. In the kidney of *Ostα*$^{-/-}$ mice after BDL the apical bile acid uptake transporter, Asbt, is further reduced, while apical export transporters, Mrp2 and Mrp4, are increased, resulting in a significant increase in urinary bile acid excretion. Conclusions: These findings indicate that loss of *Ostα* provides protection from liver injury in obstructive cholestasis through adaptive responses in both the kidney and liver that enhance clearance of bile acids into urine and through detoxification pathways most likely mediated by the nuclear receptor, Car.

Keywords

adaptive regulation; urinary bile acids; nuclear receptor; kidney, bile acid homeostasis

Organic solute transporter alpha-beta (Ostα-Ostβ) is a basolateral membrane transporter that plays a key role in the enterohepatic circulation of bile acids and the homeostatic control of bile acid biosynthesis (1,2). In *Ostα* deficient mice, bile acids accumulate in the enterocyte and

Corresponding author: Carol J. Soroka, Ph.D. Senior Research Scientist Department of Medicine Yale University School of Medicine 333 Cedar Street/1080 LMP, PO Box 208019 New Haven, CT 06520-8019 Phone: 203-785-3154 Fax: 203-785-7273 carol.soroka@yale.edu.
Carol J. Soroka carol.soroka@yale.edu
Albert Mennone al.mennone@yale.edu
Lee R. Hagey lhagey@ucsd.edu
Nazzareno Ballatori Ned_Ballatori@URMC.Rochester.edu
James L. Boyer james.boyer@yale.edu

NIH-PA Author Manuscript
NIH-PA Author Manuscript
NIH-PA Author Manuscript

NIH-PA Author Manuscript

NIH-PA Author Manuscript

NIH-PA Author Manuscript

up-regulate fibroblast growth factor 15 (*Fgf15*) via farnesoid X receptor (Fxr) dependent mechanisms (3,4). Fgf15 circulates to the liver, where it binds to the Fgf receptor 4 (FgfR4), activating a kinase-mediated signal transduction pathway that results in feed back down-regulation of bile acid synthesis by Cyp7a1 (5). This results in a significant decrease in the bile acid pool size, although the composition of the pool is not altered (2). Fecal bile acid excretion remains normal, whereas fecal cholesterol is increased ~4 fold (1,2).

In the rodent, the highest level of expression of Ostα-Ostβ is in the ileum, the renal proximal tubules, and the adrenal gland (3,4,6,7). Unlike humans, rodents have practically undetectable levels of Ostα-Ostβ in the liver (3,4). However, in cholestatic conditions, the accumulation of bile acids in the liver results in increased expression of Ostα-Ostβ at the sinusoidal membrane, where it is in a position to facilitate extrusion of toxic bile acids and other sterols into the circulation as part of the adaptive protective response to cholestatic liver injury (8,9).

Much of our knowledge about the response to cholestatic injury comes from rodent animal models, particularly common bile duct ligation (BDL). After BDL the liver attempts to prevent injury by limiting uptake of bile acids from the circulation, decreasing bile acid biosynthesis, and increasing export of bile acids out of the liver, largely through the hepatic basolateral membrane transporters, Mrp3, Mrp4 and Ostα-Ostβ (10,11). Previous studies in mice genetically deficient for Mrp3 have shown that the lack of Mrp3 results in no change in liver injury after BDL and no difference in serum or urinary levels of bile acids (12,13). In contrast, mice deficient in Mrp4 develop more severe liver injury and lower serum bile acid levels after BDL than wild-type mice (14) suggesting that up-regulation of Mrp3 and Ostα-Ostβ are not able to fully compensate for the loss of Mrp4. In the present study, we have now examined the potential contribution of Ostα-Ostβ to the adaptive response to BDL in *Ostα* deficient mice. Surprisingly, our data indicate that Ostα deficiency results in a substantial protective effect to the bile duct obstructed liver, in association with a previously unsuspected augmentation in the urinary excretion of bile acids. Thus, strategies to inhibit renal Ostα-Ostβ may provide a novel approach to treatment of cholestatic liver disease

Experimental Procedures

Animals

Ostα$^{-/-}$ mice were generated as previously described (1,15). All animals were housed in a temperature- and humidity-controlled environment under a constant light cycle where they had free access to water and food. BDL was performed under sterile conditions as previously described from this laboratory (16,17). Control animals (wild-type C57Bl/6) underwent sham surgery in which the bile duct was exposed, but not ligated. Tissue, plasma, bile (from the gallbladder) and urine (from the urinary bladder) were collected 7 days after surgery. Mice were fasted overnight and all animals were sacrificed between 8 and 11 am. Tissues were flushed free of blood, snap frozen in liquid nitrogen and stored at −80°C until used.

All experimental protocols were approved by the local Animal Care and Use Committee, according to criteria outlined in the “Guide for the Care and Use of Laboratory Animals” prepared by the National Academy of Sciences, as published by the National Institutes of Health (NIH publication 86-23, revised 1985).

Quantitation of serum and tissue components

Quantitation of total bilirubin, aminotransferase (ALT), and γ–glutamyl-transpeptidase (γGT) were performed using kits from Thermo Fisher Scientific (Cincinnati, OH). Quantitation of 3α-hydroxybile acids was done with a kit from Trinity BioTech (Newark, NJ). Hepatic levels of hydroxyproline were measured according to Fickert et al (18).

NIH-PA Author Manuscript

NIH-PA Author Manuscript

NIH-PA Author Manuscript

Bile acid analysis

Liver extracts and urine samples were dissolved in methanol/1% isopropanol, centrifuged, and analyzed by nanoESI-MS. The instrument was a Perkin-Elmer Sciex API-III (Perkin-Elmer, Alberta, Canada) modified with a nanoelectrospray source from Protana A/S (Odense, Denmark). Borosilicate glass capillaries (Protana) were used for sample injection. The instrument was operated in the negative mode. Chemical identity of the peaks was confirmed by the fragmentation pattern of selected ion (Q3 mode) using argon gas. Conjugates giving rise to sulfate (m/z 97) and taurine(m/z 124) were identified.

Histology and Cytokeratin 19 Immunohistochemistry

Formalin fixed tissue was paraffin embedded and sections were stained with hematoxylin and eosin, Masson trichrome, and Sirius Red. Immunohistochemistry was performed on additional sections using antibody to cytokeratin 19 (Troma-III) developed by R. Kemler and obtained from the Developmental Studies Hybridoma Bank developed under the auspices of the NICHD and maintained by The University of Iowa, Department of Biological Sciences, Iowa City, IA using a DAB peroxidase kit (Vector Laboratory, Burlingame, CA). Quantitation of cytokeratin 19 labeling was performed using ImageJ software (NIH open source) with thresholding. Data are presented as a percentage of the total area that is positive for cytokeratin 19.

Real-Time RT-PCR

Total RNA was isolated from tissue using Trizol reagent (Invitrogen, Grand Island, NY) and reverse transcribed using Pro-Star First Strand kit (Stratagene, La Jolla, CA). Quantitative PCR was performed using Applied Biosystems' 7500 DNA Sequence Detector System (Applied Biosystems, Foster City, CA). Specific primer pairs and probes were purchased (TaqMan Gene Expression Assays, Applied Biosytems) and data normalized to Gapdh expression.

Western blotting

Protein expression was determined in whole cell lysates (Car, Pxr, Sult2a1) or in total membrane fractions prepared as previously described (8). Primary antibodies (Supplemental Table S1) were incubated overnight at 4°C. Horseradish peroxidaseconjugated secondary antibodies were from Sigma (St. Louis, MO) and enhanced chemiluminescence reagents were from Amersham Pharmacia Biotech (Piscataway, NJ). Densitometry was performed using the Fotodyne System (FotoDyne Incorp, Hartland, WI).

Statistics

All data represent mean ± standard deviation based on Student's t-test for 4–6 animals per group. For simplicity in Figures 4, 5 and 6, significance is shown as $p<0.05$, although in many cases the significance is greater.

Results

Ostα$^{-/-}$ mice are protected from cholestasis

Following surgery all animals demonstrated similar changes in body weight, liver weight and kidney weight. As previously noted (1,2), the small intestine of *Ostα*$^{-/-}$ mice were longer and this difference was maintained after BDL (data not shown). Serum levels of cholestatic markers (ALT, γGT, bile acids and bilirubin) were all substantially lower in the *Ostα*$^{-/-}$ mice after BDL compared to *Ostα*$^{+/+}$ mice, suggesting that *Ostα* deficient mice were protected from cholestatic injury (Table 1). Blinded analysis of histologic sections of liver suggested less fibrosis and bile duct proliferation, but similar amounts of necrosis and inflammation between *Ostα*$^{+/+}$ and *Ostα*$^{-/-}$ BDL mice (Figure 1A and Supplement Figure 1S). QPCR confirmed lower levels of liver mRNA for procollagen I and transforming growth factor beta (TGFβ1), and

NIH-PA Author Manuscript

NIH-PA Author Manuscript

NIH-PA Author Manuscript

hydroxyproline levels were significantly lower in *Ostα*$^{-/-}$ BDL mouse liver (Figure 1B–D). Morphometric analysis of cytokeratin 19 staining of liver sections demonstrated less, but not statistically significant (p=0.06), bile duct proliferation in *Ostα*$^{-/-}$ BDL mice (Figure 1E and F).

Consistent with this protective effect, hepatic bile acid concentrations were significantly less in BDL *Ostα*$^{-/-}$ mice (Figure 2A). Surprisingly, urinary bile acid concentrations were significantly increased as compared to *Ostα*$^{+/+}$ BDL mice (Figure 2D). The biliary and renal parenchymal bile acids levels were unchanged (Figure 2B and E). However, bilirubin levels were increased ~ 5 fold in the bile and decreased in the renal parenchyma when compared to *Ostα*$^{+/+}$ mice after BDL (Figure 2C and F). Additional bile collection studies in untreated *Ostα*$^{+/+}$ and *Ostα*$^{-/-}$ mice revealed that bile flow and bile acid excretion were slightly lower in the *Ostα* deficient mice, but bile acid, cholesterol, and phospholipid concentrations were not significantly different over a 90 minute collection period (Supplement Figure S2).

Mass spectrometric analysis of the liver tissue revealed no difference in the bile acid composition between sham *Ostα*$^{+/+}$ and *Ostα*$^{-/-}$ mice (Figure 3A). However, after BDL there was a 35-fold increase in tetrahydroxy bile acids in the *Ostα*$^{+/+}$ liver tissue that was not seen in the *Ostα*$^{-/-}$ mice (Figure 3A). Spectrometric analysis of the urine revealed significant accumulation of tetrahydroxylated bile acids (~40%) and some pentahydroxylated bile acids (~3.5%) and glucuronides (2.75%) in the *Ostα*$^{+/+}$ BDL mice. In contrast, the *Ostα*$^{-/-}$ BDL mouse urine had limited tetrahydroxylated bile acids (~10%) and no pentahydroxylated bile acids or glucuronides. Interestingly, the *Ostα*$^{-/-}$ mouse livers showed a significantly greater accumulation of bile alcohol sulfates than in the *Ostα*$^{+/+}$ mice after BDL (Figure 3B). Similarly, *Ostα*$^{-/-}$ BDL mice had 4.5 times more urinary excretion of sulfated bile alcohols than *Ostα*$^{+/+}$ BDL mice (Table 1). The difference in hepatic and urine bile acid composition may be due to less bile acid accumulation in *Ostα*$^{-/-}$ mice because of the lower starting bile acid pool, as well as greater hepatic and urine bile acid clearance.

Adaptive regulation in the liver after BDL

We next determined whether there was a difference in the adaptive response of genes for several nuclear receptors and for bile acid uptake, synthesis, detoxification, and secretion. In contrast to the wild-type BDL mice, mRNA levels for the nuclear receptors, *Fxr* and *Pxr*, were unchanged after BDL in the *Ostα*$^{-/-}$ mice (Figure 4A). However, *Car* mRNA levels, which were unchanged in the wild-type mice after BDL, were significantly higher in both the sham and BDL *Ostα*$^{-/-}$ mice (Figure 4A). In addition, the *Ostα*$^{-/-}$ BDL mice had significantly higher mRNA levels for *Cyp7a1*, *Cyp2b10*, *Cyp3a11*, sulfotransferase 2a1 (*Sult2a1*), and UDP-glucuronosyltransferase 1a1 (*Ugt1a1*), compared to *Ostα*$^{+/+}$ BDL mice (Figure 4B). Protein expression levels for Car and Sult2a1 were elevated after BDL in the *Ostα*$^{-/-}$ mice (although not quite significant for Car, p=0.054), while Pxr protein expression was significantly decreased in both *Ostα*$^{+/+}$ and *Ostα*$^{-/-}$ mice after BDL (Figure 4C). Small heterodimer partner (*Shp*) and *FgfR4* mRNA levels in the liver were lower in *Ostα*$^{-/-}$ BDL mice compared to *Ostα*$^{+/+}$ BDL mice (Figure 4A). Consistent with total obstruction of bile flow into the intestine, both groups of BDL animals demonstrated a significant decrease in intestinal production of *Fgf15* (only 6% of the sham levels, data not shown). The decrease in *Fgf15* and *Shp* and the increase in *Cyp7a1* suggest that, unlike the *Ostα*$^{+/+}$ BDL mice, bile acid synthesis is actually increased in the *Ostα* deficient BDL mice. This conclusion is supported by estimates of the bile acid pool size in the BDL animals (sum of bile acids in serum, liver, kidney and bile) that indicate that *Ostα*$^{-/-}$ mice have a pool size that is 54% of the *Ostα*$^{+/+}$ mice (Table 1), which is considerably higher than previously reported (10–35%) in *Ostα*$^{-/-}$ mice (1, 2).

Expression of key membrane transporters in the liver and kidney was determined by QPCR and Western blotting to further assess the adaptive response. In the liver of wild-type mice

NIH-PA Author Manuscript

NIH-PA Author Manuscript

NIH-PA Author Manuscript

after BDL there was an increase in the mRNA levels of the basolateral efflux transporter, *Mrp4*, but no change in *Mrp3* or the two canalicular apical membrane proteins, *Mrp2* and bile salt export pump (*Bsep*) (Figure 5A). In contrast, in *Ostα*$^{-/-}$ mouse liver, *Mrp 4*, *Mrp3*, and *Bsep* mRNA were increased after BDL (Figure 5A). Interestingly, sham *Ostα*$^{-/-}$ mice had increased levels of Mrp2 mRNA and decreased mRNA for Bsep compared to sham wild-type mice (Figure 5A). Following BDL, the increase in mRNA for *Bsep* in *Ostα*$^{-/-}$ mice is consistent with an increase in bile acid synthesis and hepatic bile acid levels in these animals.

Western blotting of liver membrane proteins demonstrated that, in the wild-type mice, Mrp3, but not Mrp4 or Mrp2, were higher after BDL (Figure 5B). However, all three membrane proteins were higher after BDL in the *Ostα*$^{-/-}$ mice (Figure 5B). In addition, although the basolateral uptake protein, Oatp1a1, was almost undetectable after BDL in the wild-type mice, it was expressed at significantly higher levels in the *Ostα* deficient mice after BDL (Figure 5B). The other bile acid uptake protein, sodium dependent taurocholate co-transporting polypeptide (Ntcp) was significantly down in both groups of BDL mice (Figure 5B). Although *Mrp2* mRNA level was higher in sham *Ostα*$^{-/-}$ mice compared to the sham wild-type mice, the protein expression for this apical transporter was very low in these sham *Ostα* deficient mice, suggesting instability of the protein. However, after BDL the protein expression is increased to wild-type level (Figure 5B) and bilirubin concentration in the bile is significantly increased (Figure 2C).

Adaptive regulation in the kidney after BDL

Adaptive responses to cholestasis also occur in the kidney in an effort to eliminate excess bile acids and toxic compounds from the circulation. In the kidney of *Ostα*$^{+/+}$ mice, only mRNA levels for *Mrp3* were significantly changed after BDL (Figure 6A). However, in kidneys of *Ostα*$^{-/-}$ mice, mRNA levels for *Mrp2*, *Mrp3* and *Mrp4* and protein expression of Mrp2 and Mrp4 were all higher (Figure 6A and B). In contrast, mRNA for the apical sodium dependent bile salt transporter, *Asbt*, which was lower in sham *Ostα*$^{-/-}$ mice, remained low after BDL (Figure 6A), while Asbt protein became essentially undetectable (Figure 6B). These changes in renal bile acid transporters after BDL, in the absence of Ostα, function to severely limit the uptake of bile acids from the tubular lumen and enhance their excretion, thereby significantly augmenting bile acid clearance in the urine.

Discussion

Cholestatic liver disease is characterized by retention of bile that leads to pathological changes, including bile duct proliferation, apoptosis/necrosis, and fibrosis, that often progress to liver failure and the need for liver transplantation. As a consequence, adaptive responses occur in the liver that attempt to minimize bile acid accumulation and toxicity by decreasing bile acid uptake and synthesis, metabolizing bile acids to less toxic moieties, and up-regulating the expression of basolateral membrane export pumps in an attempt to extrude bile acids back into the systemic circulation (10,11,19). This latter process is facilitated by three important bile acid and organic solute transporters: Mrp3, Mrp4, and Ostα-Ostβ. A clearer understanding of the regulation of each of these transporters is necessary for development of new therapeutic interventions for cholestasis. Because there is some overlap in the substrate specificities of these basolateral export proteins, much of the work has depended upon the development of mice genetically deficient in each of the proteins. To date, only two of these export pumps (Mrp3 and Mrp4) have been studied with models of cholestasis in genetically null mice (12–14). Unlike Mrp3 null mice, mice lacking Mrp4 demonstrated more severe liver injury than wild-type controls, suggesting a more essential role for Mrp4 in the export of toxic bile acids (14). Here we present the first study of cholestasis in mice deficient in the third protein, Ostα, an obligate partner of the heteromeric, facilitated transporter of bile acids and organic

NIH-PA Author Manuscript

NIH-PA Author Manuscript

NIH-PA Author Manuscript

sterols, Ostα-Ostβ. We demonstrate that in the absence of *Ostα*, the liver paradoxically is partially protected from the accumulation of hepatic bile acids and subsequent development of hepatic fibrosis and that this protection is accompanied by an augmentation of bile acid excretion in the urine.

Recent studies have characterized the phenotype of the *Ostα*$^{-/-}$ mouse models (1,2) and demonstrated that ileal Ostα-Ostβ plays a key role in the enterohepatic circulation of bile acids. These studies showed that in the absence of intestinal Ostα-Ostβ, bile acids accumulate in the intestine, up-regulating Fgf15 via Fxr, which results in feed back down-regulation of bile acid synthesis by Cyp7a1 and a smaller bile acid pool (2). These findings are not characteristic of mice genetically null for Mrp4 or Mrp3 (12,13,20) and highlight the importance of ileal Ostα-Ostβ as a regulator of normal bile acid homeostasis. As might be expected with such a small bile acid pool, the *Ostα*$^{-/-}$ mice show less accumulation of hepatic bile acids after BDL, especially of polyhydroxylated forms. However, because obstructive cholestasis in these animals prevents bile acids from entering the intestine, there is a loss of signaling from Fgf15 and a lowering of the elevated liver levels of *Shp* and *FgfR4* mRNA that otherwise occur in wild-type BDL mice. Thus, *Cyp7a1* and *Bsep* are up-regulated and the bile acid pool is increased.

Fxr, Car and Pxr are all key nuclear receptors that participate in the adaptive response to cholestatic injury (21,22). Car and Pxr play important roles in bile acid detoxifying enzymes in mice and in the regulation of Mrp4 and Sult2a1 (23,24,25). However, unlike Fxr or Pxr we find that sham and BDL *Ostα* deficient mice have a significant increase in *Car* mRNA compared to the wild-type controls, suggesting that this nuclear receptor may play a more important regulatory role in detoxification in these mice. Our data are consistent with Car induced Phase I (Cyp3a11, Cyp2b10) and Phase II (Sult2a1, Ugt1a1) detoxification enzymes (24,25). Furthermore, they support the concept that this nuclear receptor can induce expression of the Phase III transporters, Mrp3 and Mrp4, and provide alternative pathways for bile acid export from the liver (24).

Another particularly novel finding in this study is that in the absence of *Ostα*, obstructive cholestasis leads to a further increase in urinary excretion of bile acids than otherwise occurs in cholestasis. This has also been shown in mice treated with Car agonists and subjected to 24 hr BDL (24). We show that adaptive regulation of key membrane transporters in the kidney could be responsible for this change. First, in the absence of Ostα-Ostβ in the proximal tubule, *Ostα* deficient mice cannot reabsorb the increase in urinary filtration of bile acids that occurs after BDL. Second, the renal apical uptake transporter, Asbt, is further decreased and the renal apical export transporters, Mrp2 and Mrp4, are both increased. Thus, bile acids are blocked from being transported back to the systemic circulation and the limited amount that are taken up into the proximal tubule, are effectively exported back out the apical membrane into the urine. This conclusion is also supported by the finding of increased urinary excretion of the Ostα-Ostβ substrates [^{3}H] estrone 3-sulfate and [^{3}H] dehydroepiandrosterone sulfate when administered to *Ostα*$^{-/-}$ mice (1).

In summary, liver injury is attenuated in *Ostα*$^{-/-}$ mice following BDL. We show in this study that this paradoxical protective effect is associated with, and thus presumably mediated by, changes in bile acid metabolism and transport in the intestine, liver and kidney (Figure 7). The genetic deletion of Ostα leads first to alterations in bile acid homeostasis, increasing formation of Fgf15 and inhibition of *Cyp7a1*, resulting in a smaller bile acid pool size in these animals (1,2). When these animals are subjected to BDL, the endocrine actions of Fgf15 are eliminated because bile acids are now excluded from the intestine, resulting in up-regulation of bile acid synthesis and hepatic basolateral membrane bile acid export transporters. Finally, the inability of the kidney to reabsorb bile acids because of the absence of Ostα in association with further

NIH-PA Author Manuscript

NIH-PA Author Manuscript

NIH-PA Author Manuscript

down-regulation of Asbt and up-regulation of renal Mrp2 and Mrp4, all result in a significant escape route for bile acids in the urine that does not normally occur to this extent in the conventional adaptive response of the kidney to cholestasis. This finding has significant therapeutic implications because strategies to down-regulate Ostα in the kidney should have major clinical benefits in cholestatic liver injury by further augmenting the renal excretion of bile acids and thus diminishing their hepatic and systemic accumulation as shown in this study.

Supplementary Material

Refer to Web version on PubMed Central for supplementary material.

Acknowledgments

We thank Kathy Harry for technical assistance and Christine L. Hammond for help with the collection and analysis of hepatic bile.

This work was supported by National Institute of Health Research Grants DK 25636 and DK34989 (to JLB) and DK067214 (to NB)

Abbreviations

Ostα-Ostβ	organic solute transporter alpha-beta
BDL	bile duct ligation
Car	constitutive androstane receptor
Cyp	cytochrome P450
Sult2a1	sulfotransferase 2a1
Ugt1a1	UDP-glucuronosyltransferase 1a1
Mrp	multidrug resistance-associated protein
Fgf15	fibroblast growth factor 15
Fxr	farnesoid X receptor
FgfR4	fibroblast growth facter receptor 4
ALT	aminotransferase
γGT	γ-glutamyl-transpeptidase
TGFβ	transforming growth factor beta
Pxr	pregnane X receptor
Shp	small heterodimer partner
Bsep	Bile salt export pump
Ntcp	sodium dependent taurocholate co-transporting polypeptide
Asbt	apical sodium dependent bile salt transporter

References

1. Ballatori N, Fang F, Christian WV, Li N, Hammond CL. Ostα-Ostβ is required for bile acid and conjugated steroid disposition in the intestine, kidney, and liver. Am J Physiol Gastrointest Liver Physiol 2008;295:G179–186. [PubMed: 18497332]

NIH-PA Author Manuscript

NIH-PA Author Manuscript

NIH-PA Author Manuscript

2. Rao A, Haywood J, Craddock AL, Belinsky MG, Kruh GD, Dawson PA. The organic solute transporter α-β, Ostα-Ostβ, is essential for intestinal bile acid transport and homeostasis. PNAS 2008;105:3891–3896. [PubMed: 18292224]
3. Ballatori N, Christian WV, Lee JY, Dawson PA, Soroka CJ, Boyer JL, Madejczyl MS, et al. OSTα-OSTβ: A Major Basolateral Bile Acid and Steroid Transporter in Human Intestinal, Renal, and Biliary Epithelia. Hepatology 2005;42:1270–1279. [PubMed: 16317684]
4. Dawson PA, Hubbert HJ, Craddock AL, Zeranque N, Christian WV, Ballatori N. The heteromeric organic solute transporter alpha-beta, Ostα-Ostβ, is an ileal basolateral bile acid transporter. J Biol Chem 2005;280:6960–6968. [PubMed: 15563450]
5. Inagaki T, Choi M, Moschetta A, Peng L, Cummins CL, McDonald JG, Luo G, et al. Fibroblast growth factor 15 functions as an enterohepatic signal to regulate bile acid homeostasis. Cell Metabolism 2005;2:217–225. [PubMed: 16213224]
6. Seward DJ, Koh AS, Boyer JL, Ballatori N. Functional Complementation between a Novel Mammalian Polygenic Transport Complex and an Evolutionarily Ancient Organic Solute Transporter, *OST*α-*OST*β. J Biolo Chem 2003;278:27473–27482.
7. Wang W, Seward DJ, Li L, Boyer JL, Ballatori N. Expression cloning of two genes that together mediate organic solute and steroid transport in the liver of a marine vertebrate. PNAS 2001;98:9431–9436. [PubMed: 11470901]
8. Boyer JL, Trauner M, Mennone A, Soroka CJ, Cai S-Y, Mounstafa T, Zollner G, et al. Upregulation of a Basolateral RXR-dependent bile acid efflux transporter OSTα-OSTβ in Cholestasis in Humans and Rodents. Am J Physiol Gastrointest Liver Physiol 2006;290:G1124–G1130. [PubMed: 16423920]
9. Zollner G, Wagner M, Mounstafa T, Ficket P, Silbert D, Gumhold J, Fuchsbichler A, et al. Coordinated Induction of Bile Acid Detoxification and Alternative Elimination in Mice: Role of FXR-regulated Organic Solute Transporter-α/β in the Adaptive Response to Bile Acids. Am J Physiol Gastrointest Liver Physiol 2006;290:G923–G932. [PubMed: 16357057]
10. Boyer JL. New perspectives for the treatment of cholestasis: lessons from basic science applied clinically. Journal of Hepatology 2007;46:365–371. [PubMed: 17223219]
11. Kosters A, Karpen SJ. Bile acid transporters in health and disease. Xenobiotica 2008;38:1043–1071. [PubMed: 18668439]
12. Belinsky MG, Dawson PA, Shchaveleva I, Bain LJ, Wang R, Ling V, Chen Z-S, et al. Analysis of the in vivo functions of Mrp3. Molecular Pharmacology 2005;68:160–168. [PubMed: 15814571]
13. Zelcer N, van de Wetering K, de Waart R, Scheffer GL, Marschall H-U, Wielinga PR, Kuil A, et al. Mice lacking Mrp3 (Abcc3) have normal bile salt transport, but altered hepatic transport of endogenous glucuronides. Journal of Hepatology 2006;44:768–775. [PubMed: 16225954]
14. Mennone A, Soroka CJ, Cai S-Y, Harry K, Adachi M, Hagey L, Schuetz JD, et al. Mrp4 -/- Mice have an Impaired Cytoprotective Response in Obstructive Cholestasis. Hepatology 2006;43:1013–1021. [PubMed: 16628672]
15. Li N, Cui Z, Fang F, Lee JY, Ballatori N. Heterodimerization, trafficking and membrane topology of the two proteins, Ostα and Ostβ, that constiture the organic solute and steroid transporter. Biochem J 2007;407:363–372. [PubMed: 17650074]
16. Gartung C, Ananthanarayanan M, Rahman M, Schuele S, Nundy S, Soroka CJ, Stolz A, et al. Down-regulation of expression and function of the rat liver Na+/bile acid cotransporter in extrahepatic cholestasis. Gastroenterology 1996;110:199–209. [PubMed: 8536857]
17. Trauner M, Arrese M, Soroka CJ, Ananthanarayannan M, Koeppel T, Schlosser S, Suchy FJ, et al. The rat canalicular conjugate export pump (mrp2) is down-regulated in intrahepatic and obstructive cholestasis. Gastroenterology 1997;113:255–264. [PubMed: 9207286]
18. Fickert P, Fuchsbichler A, Marschall H-U, Wagner M, Zollner G, Krause R, Zatloukal K, et al. Lithocholic acid feeding induces segmental bile duct obstruction and destructive cholangitis in mice. American Journal of Pathology 2006;168:410–422. [PubMed: 16436656]
19. Kullak-Ublick GA, Stieger B, Meier PJ. Enterohepatic bile salt transporters in normal physiology and liver disease. Gastroenterology 2004;126:322–342. [PubMed: 14699511]
20. Leggas M, Adachi M, Scheffer GL, Sun D, Wielinga P, Du G, Mercer KE, et al. Mrp4 confers resistance to topotecan and protects the brain from chemotherapy. Molecular & Cellular Biology 2004;24:7612–7621. [PubMed: 15314169]

NIH-PA Author Manuscript

NIH-PA Author Manuscript

NIH-PA Author Manuscript

21. Guo GL, Lambert G, Negishi M, Ward JM, Brewer HB Jr. Kliewer SA, Gonzalez FJ, et al. Complementary roles of farnesoid X receptor, pregnane X receptor, and constitutive androstane receptor in protection against bile acid toxicity. Journal of Biological Chemistry 2003;278:45062–45071. [PubMed: 12923173]

22. Stedman CAM, Liddle C, Coulter SA, Sonoda J, Alvarez JGA, Moore DD, Evans RM, et al. Nuclear receptors constitutive androstane receptor and pregnane X receptor ameliorate cholestatic liver injury. Proceedings of the National Academy of Sciences of the United States of America 2005;102:2063–2068. [PubMed: 15684063]

23. Saini SPS, Sonoda J, Xu L, Toma D, Uppal H, Mu Y, Ren S, et al. A novel constitutive androstane receptor-mediated and CYP3A-independent pathway of bile acid detoxification. Molecular Pharmacology 2004;65:292–300. [PubMed: 14742670]

24. Wagner M, Halilbasic E, Marschall H-U, Zollner G, Fickert P, Langner C, Zatloukal K, et al. CAR and PXR agonists stimulate hepatic bile acid and bilirubin detoxification and elimination pathways in mice. Hepatology 2005;42:420–430. [PubMed: 15986414]

25. Assem M, Schuetz EG, Leggas M, Sun D, Yasuda K, Reid G, Zelcer N, et al. Interactions between hepatic Mrp4 and Sult2a as revealed by the constitutive androstane receptor and Mrp4 knockout mice. Journal of Biological Chemistry 2004;279:22250–22257. [PubMed: 15004017]

NIH-PA Author Manuscript

NIH-PA Author Manuscript

NIH-PA Author Manuscript

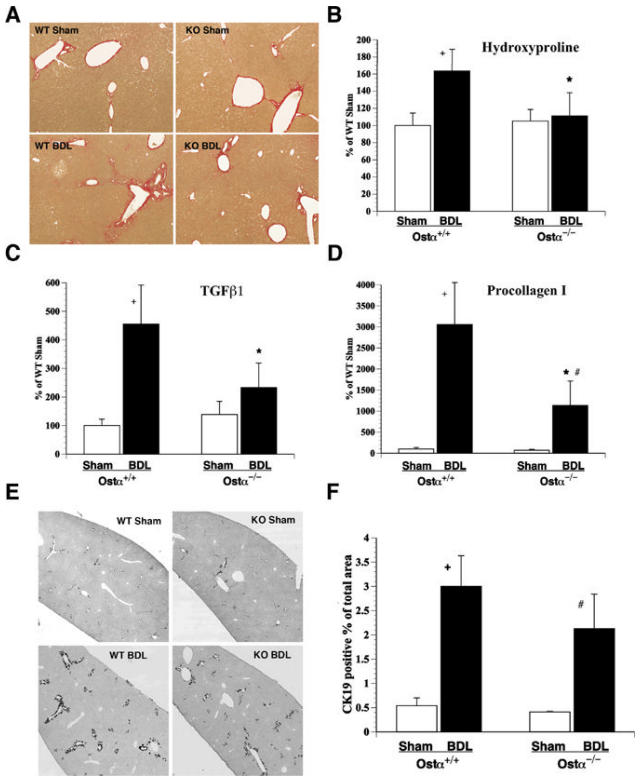

Figure 1.

BDL results in less fibrosis in the livers of *Ostα*$^{-/-}$ mice than the *Ostα*$^{+/+}$ controls. A. Sirius Red staining of liver sections. B. Hydroxyproline levels. 100%=157.50 mg/gm liver. C. mRNA for TGFβ1 is significantly increased in the *Ostα*$^{+/+}$, but not *Ostα*$^{-/-}$, mouse livers after BDL. D. mRNA levels of procollagen I are significantly lower in the *Ostα*$^{-/-}$ mice compared to the *Ostα*$^{+/+}$ mice. E. Immunohistochemical staining for bile ducts using an antibody to cytokeratin 19. WT, wild-type; KO, knockout. F. Quantitation of cytokeratin 19 revealed less bile duct proliferation in the *Ostα*$^{-/-}$ mice, although this did not reach statistical significance (p=0.06). n=5–6; +p<0.01 *Ostα*$^{+/+}$ Sham VS *Ostα*$^{+/+}$ BDL; *p<0.05 *Ostα*$^{+/+}$ BDL VS *Ostα*$^{-/-}$ BDL; #p<0.01 *Ostα*$^{-/-}$ Sham VS *Ostα*$^{-/-}$ BDL

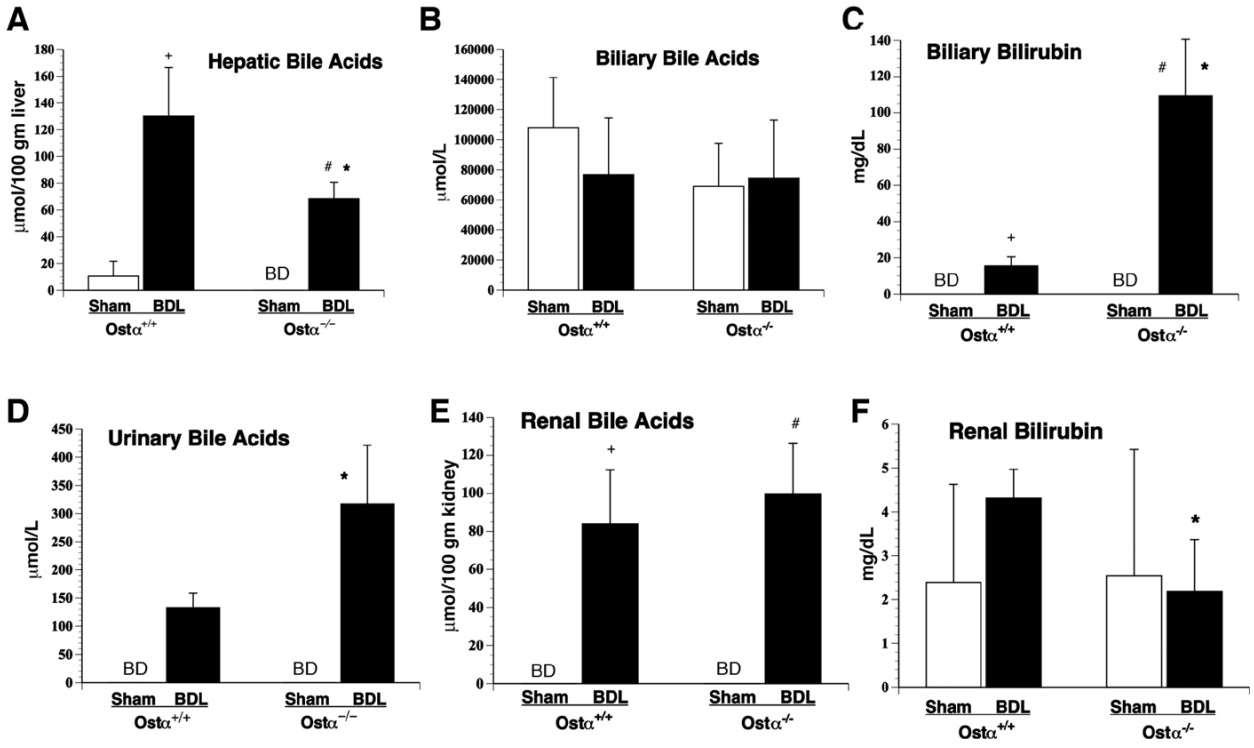

Figure 2.

Altered levels of hepatic and renal bile acids and bilirubin after BDL reflect adaptive changes that result in less hepatic retention and more urinary elimination of bile acids in *Ostα*$^{-/-}$ mice. A. Hepatic bile acids. B. Biliary bile acids. C. Biliary bilirubin. D. Urinary bile acids. E. Renal parenchymal bile acids. F. Renal parenchymal bilirubin. n=5–6; p<0.01, + *Ostα*$^{+/+}$ Sham VS *Ostα*$^{+/+}$ BDL; * *Ostα*$^{+/+}$ BDL VS *Ostα*$^{-/-}$ BDL; # *Ostα*−/− Sham VS *Ostα*$^{-/-}$ BDL; BD, below detection

NIH-PA Author Manuscript NIH-PA Author Manuscript NIH-PA Author Manuscript

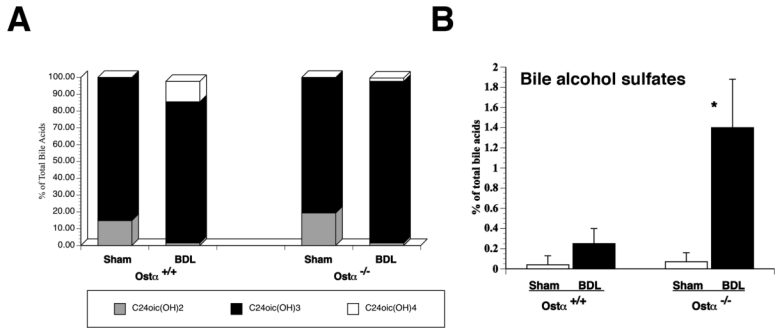

Figure 3.

Analysis of liver bile acids by mass spectrometry. A. Quantification of di-, tri-, and tetra-hydroxylated bile acids was normalized to the total detectable bile acids for each animal. After BDL, *Osta*$^{+/+}$ mice demonstrated a 35-fold increase in tetrahydroxylated bile acid which was not seen in the *Osta*$^{-/-}$ mice. B. Livers from *Osta*$^{-/-}$ mice contain significantly more bile alcohol sulfates than the *Osta*$^{+/+}$ mice. n=5–6; *p<0.001 *Ostα*$^{+/+}$ BDL VS *Ostα*$^{-/-}$ BDL

NIH-PA Author Manuscript NIH-PA Author Manuscript NIH-PA Author Manuscript

NIH-PA Author Manuscript
NIH-PA Author Manuscript
NIH-PA Author Manuscript

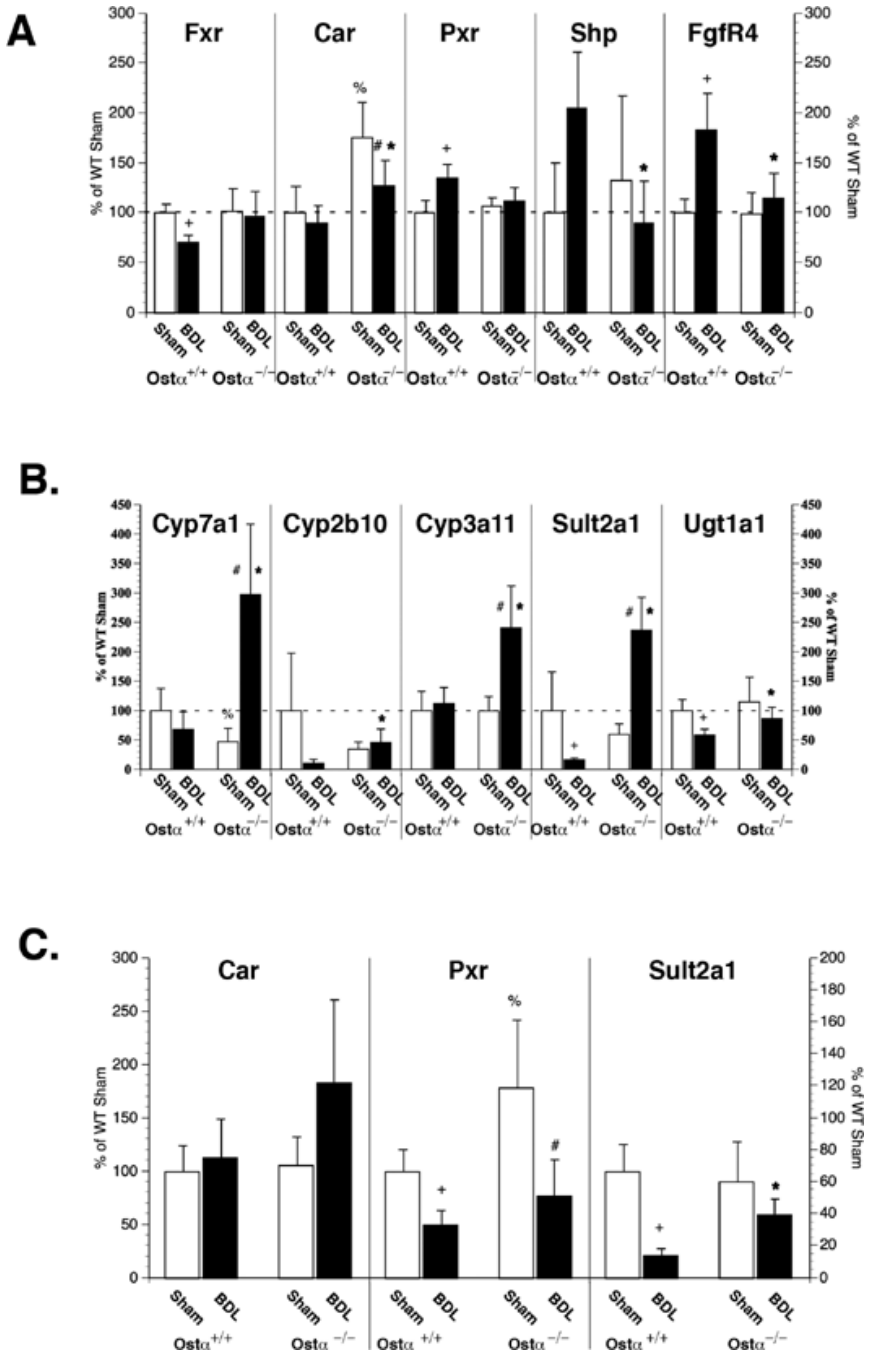

Figure 4.

Gene and protein expression in livers of sham and BDL *Ostα*$^{+/+}$ and *Ostα*$^{-/-}$ mice. A. mRNA for the nuclear receptors, *Fxr* and *Pxr*, are unchanged in *Ostα*$^{-/-}$ mice, while the xenobiotic receptor, *Car*, is significantly increased in sham and BDL *Ostα*$^{-/-}$ mice. Both *Shp* and *FgfR4* mRNA are significantly increased in the *Ostα*$^{+/+}$ BDL mice, but are lower in *Ostα*$^{-/-}$ BDL mice compared to the *Ostα*$^{+/+}$ BDL mice. B. mRNA levels are increased for *Cyp7a1*, *Cyp2b10*, *Cyp3a11*, *Sult2a1*, *Ugt1a1* in *Ostα*$^{-/-}$ BDL mice as compared to *Ostα*$^{+/+}$ BDL mice. C. Protein expression of Car and Sult2a1, but not Pxr, tend to be elevated after BDL in *Ostα*$^{-/-}$, but not *Ostα*$^{+/+}$, mice. Data are normalized to SH-PTP. n=5–6; $p<0.05$, + *Ostα*$^{+/+}$

Sham VS *Ostα*$^{+/+}$ BDL; * *Ostα*$^{+/+}$ BDL VS *Ostα*$^{-/-}$ BDL; % *Ostα*$^{+/+}$ Sham VS *Ostα*$^{-/-}$ Sham; # *Ostα*$^{-/-}$ Sham VS *Ostα*$^{-/-}$ BDL

NIH-PA Author Manuscript
NIH-PA Author Manuscript
NIH-PA Author Manuscript

NIH-PA Author Manuscript

NIH-PA Author Manuscript

NIH-PA Author Manuscript

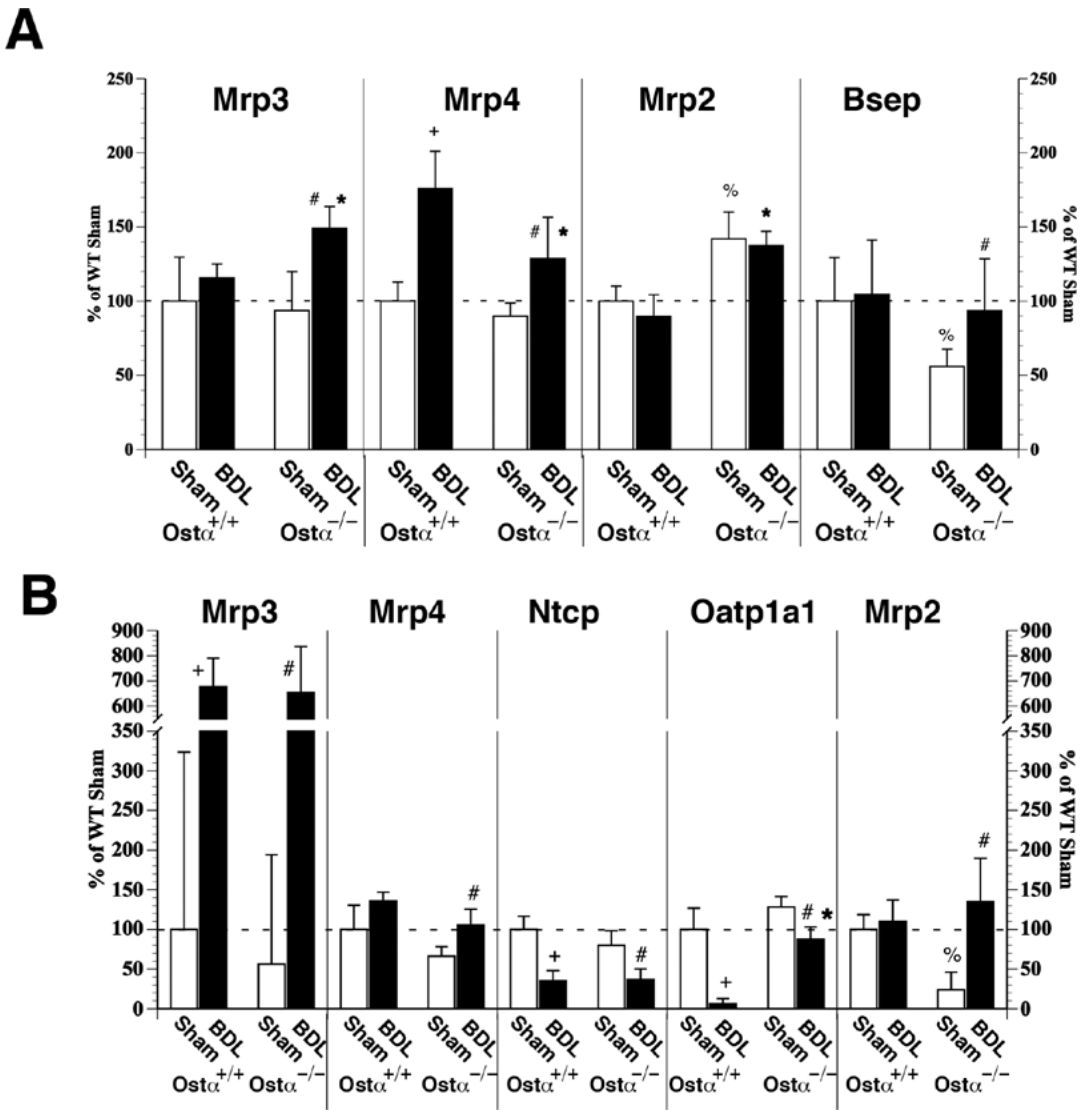

Figure 5.

Membrane transporter gene and protein expression in livers of *Ostα*$^{+/+}$ and *Ostα*$^{-/-}$ mice. A. mRNA expression. *Mrp3* and *Mrp4* are both higher in *Ostα*$^{-/-}$ BDL mice than the *Ostα*$^{-/-}$ sham controls. The apical transporter, *Mrp2*, is higher in sham and BDL *Ostα*$^{-/-}$ mice, whereas *Bsep* is decreased in the sham and then increased to wild-type levels after BDL. B. Protein expression. Mrp3 and Mrp4 is higher after BDL in *Ostα*$^{-/-}$ mice. Both Ntcp and Oatp1a1 are significantly decreased after BDL in the wild-type mice, but Oatp1a1 is maintained close to sham levels in the *Ostα*$^{-/-}$ mice. Protein expression of Mrp2 is down in the sham *Ostα*$^{-/-}$ mice, but increases after BDL. n=5–6; $p<0.05$, + *Ostα*$^{+/+}$ Sham VS *Ostα*$^{+/+}$ BDL; * *Ostα*$^{+/+}$ BDL VS *Ostα*$^{-/-}$ BDL; % *Ostα*$^{+/+}$ Sham VS *Ostα*$^{-/-}$ Sham; # *Ostα*$^{-/-}$ Sham VS *Ostα*$^{-/-}$ BDL

NIH-PA Author Manuscript

NIH-PA Author Manuscript

NIH-PA Author Manuscript

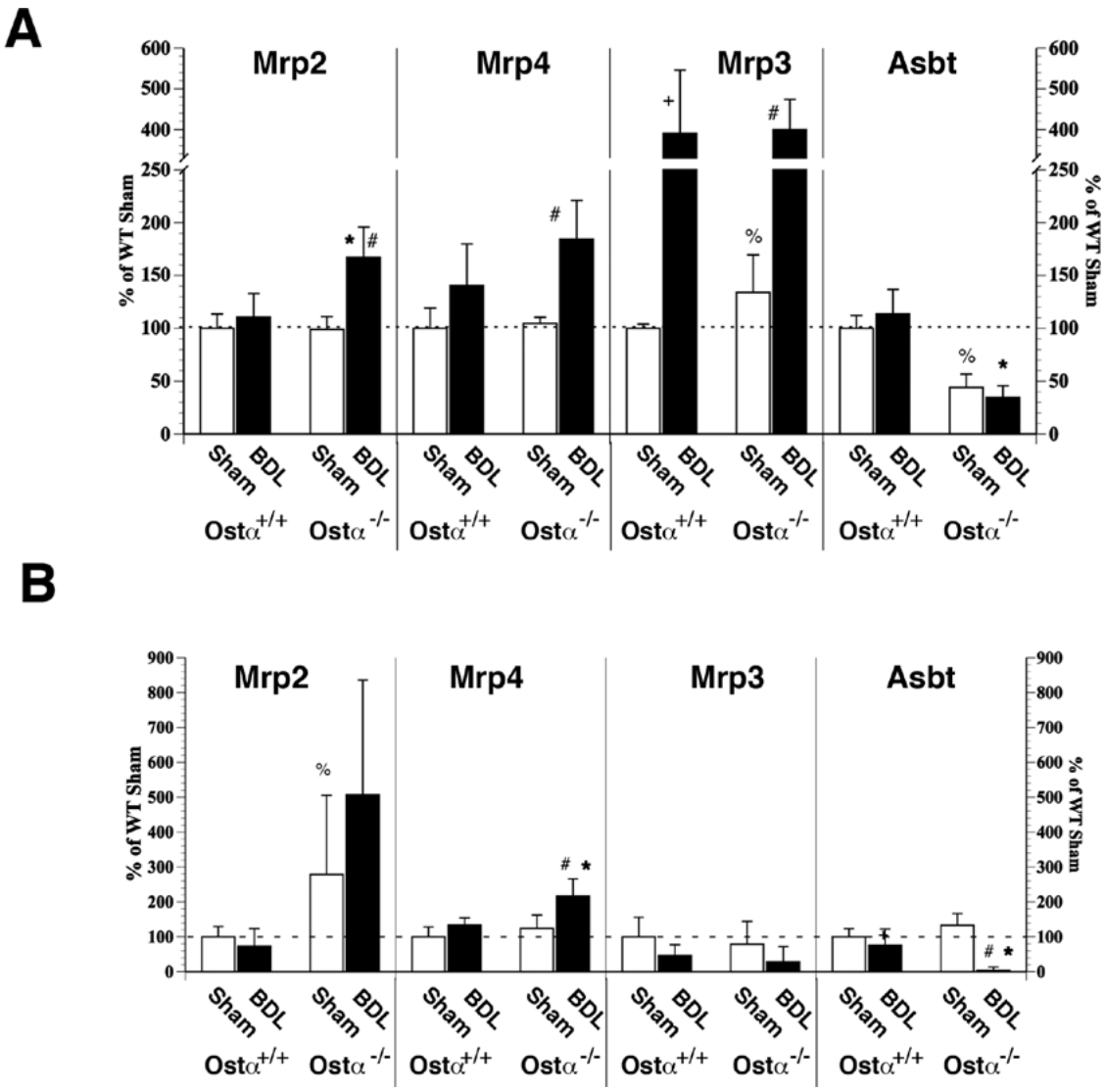

Figure 6.

Membrane transporter gene and protein expression in kidneys of $Ost\alpha^{+/+}$ and $Ost\alpha^{-/-}$ mice. A. mRNA expression. The apical export transporters, *Mrp2* and *Mrp4*, are up-regulated in the kidneys of $Ost\alpha^{-/-}$ mice after BDL. mRNA for the basolateral export transporter, *Mrp3*, is higher in the sham $Ost\alpha^{-/-}$ mice than in the sham $Ost\alpha^{+/+}$ mice, but then is increased equally in the two groups after BDL. The apical bile acid uptake transporter, *Asbt*, is down-regulated in both the sham and BDL $Ost\alpha^{-/-}$ kidneys as compared to wild-type mice. B. Protein expression. Mrp4 is significantly higher after BDL in the $Ost\alpha^{-/-}$ mice. Mrp2 has a tendency to be increased in $Ost\alpha^{-/-}$ mice after BDL,. There was no change in the basolateral Mrp3, whereas the apical uptake transporter, Asbt, was almost undetectable after BDL in the $Ost\alpha^{-/-}$ mice. All samples were normalized to β-actin. n=5–6; $p<0.05$, + $Ost\alpha^{+/+}$ Sham VS $Ost\alpha^{+/+}$ BDL; * $Ost\alpha^{+/+}$ BDL VS $Ost\alpha^{-/-}$ BDL; % $Ost\alpha^{+/+}$ Sham VS $Ost\alpha^{-/-}$ Sham; # $Ost\alpha^{-/-}$ Sham VS $Ost\alpha^{-/-}$ BDL

NIH-PA Author Manuscript

NIH-PA Author Manuscript

NIH-PA Author Manuscript

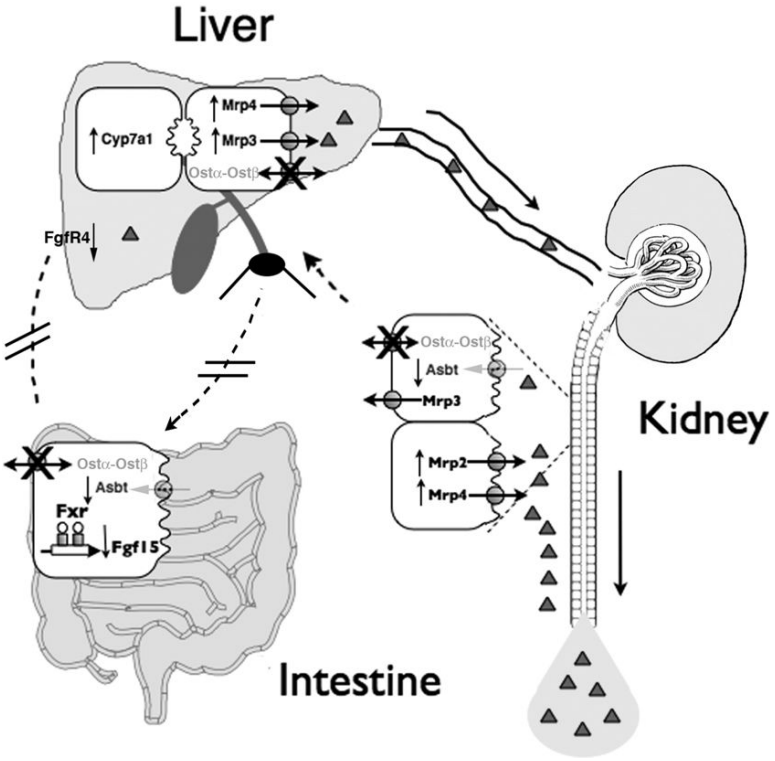

Figure 7.

Proposed protective mechanism in *Ostα*$^{-/-}$ mice after BDL. *Ostα* deficient mice have a decreased bile acid pool size and demonstrate down-regulation of the *Asbt* gene in both the intestine and kidney. After BDL, they up-regulate bile acid synthesis through lower levels of *Shp* and *Fgf15*, thereby increasing expression of *Cyp7a1*. The bile acids are transported from the liver to the circulation through an up-regulation of the basolateral transporters, Mrp3 and Mrp4, but they cannot be efficiently reabsorbed in the kidney because of the decreased expression of Asbt and the lack of Ostα-Ostβ. Furthermore, an up-regulation of the apical transporters, Mrp2 and Mrp4, efficiently prevents further accumulation of bile acids in the kidney. Therefore, ~3 fold more bile acids are excreted into the urine and removed from the body after BDL, compared to *Ostα*$^{+/+}$ mice.

NIH-PA Author Manuscript
NIH-PA Author Manuscript
NIH-PA Author Manuscript

Table 1

Serum parameters, urinary bile alcohol sulfates, and bile acid pool size of *Ostα*$^{+/+}$ and *Ostα*$^{-/-}$ mice.

	***Ostα*$^{+/+}$ sham**	***Ostα*$^{-/-}$ sham**	***Ostα*$^{+/+}$ BDL**	***Ostα*$^{-/-}$ BDL**
Serum ALT (U/L)	4.8±1.3	4.8±1.2	56.1±26.6^{+}	31.8±2.2$^{\#}$
Serum γGT (U/L)	7.6±1.7	10.8±5.0	71.6±31.2^{+}	17.8±3.3*
Serum bile acids (μM)	12.5±12.4	11.9±9.0	2023±647^{+}	371±133$^{\#*}$
Serum bilirubin (mg/dL)	0.11±0.11	0.18±0.13	23.1±9.1^{+}	6.1±1.8$^{\#*}$
Urinary bile alcohol sulfates (μM)	BD	BD	57 ± 53	258 ± 242
Bile acid pool size (μmole/100g BW)	ND	ND	61.06+15.67	33.06+14.55*

Data represent mean ± SD of n=4–6. ALT, aminotransferase; γGT, γ-glutamyl-transpeptidase; BD, below detection limit; ND, Not done

$^{+}$p<0.001, *Ostα*$^{+/+}$ Sham VS *Ostα*$^{+/+}$ BDL

$^{\#}$p<0.001, *Ostα*$^{-/-}$ Sham VS *Ostα*$^{-/-}$ BDL

*p<0.005, *Ostα*$^{+/+}$ BDL VS *Ostα*$^{-/-}$ BDL

$^{\%}$p<0.05, *Ostα*$^{+/+}$ Sham VS *Ostα*$^{-/-}$ Sham